# Recycling of perfluorosulfonic acid-based membranes and their Re-application in PEM fuel cells

Maximilian Kutter [a,f,*], Christopher Greve [b], Maximilian Maier [c,h], Monja Schilling [d], Anika Mauel [e], Annika Hilgert [a], Hendrik Hoffmann [a], Wiebke Hagemeier [a], Andreas Rosin [f], Mark Muggli [g], Roswitha Zeis [d,i,j], Jürgen Senker [e], Thomas Böhm [c], Eva M. Herzig [b], Thorsten Gerdes [f], Christina Roth [a]

[a] Electrochemical Process Engineering, Universität Bayreuth, Universitätsstraße 30, 95447, Bayreuth, Germany
[b] Herzig Group - Dynamics and Structure Formation, Institute of Physics, Universität Bayreuth, Universitätsstraße 30, 95447, Bayreuth, Germany
[c] Forschungszentrum Jülich GmbH, Helmholtz Institute Erlangen-Nürnberg for Renewable Energy (IEK-11), Cauerstr.1, 91058, Erlangen, Germany
[d] Helmholtz Institute Ulm, Karlsruhe Institute of Technology, Helmholtzstraße 11, 89081, Ulm, Germany
[e] Inorganic Chemistry III and Northern Bavarian NMR Centre, Universität Bayreuth, Universitätsstraße 30, 95447, Bayreuth, Germany
[f] Keylab Glass Technology, Universität Bayreuth, Prof.-Rüdiger-Bormann-Str. 1, 95447, Bayreuth, Germany
[g] 3M Advanced Materials Division, Dyneon GmbH, 84508, Burgkirchen an der Alz, Germany
[h] Department of Chemical and Biological Engineering, Friedrich-Alexander-Universität Erlangen-Nürnberg, Immerwahrstraße 2a, 91058, Erlangen, Germany
[i] Department of Mechanical & Industrial Engineering, University of Toronto, 5 King's College Road, Toronto, ON, M5S 3G8, Canada
[j] Department of Electrical Electronics, and Communication Engineering, Friedrich-Alexander-Universität Erlangen-Nürnberg, Cauerstraße 9, 91058, Erlangen, Germany

*Keywords:*
PFSA recycling
PFSA reprocessing
PEM fuel cells
Water retention
SAXS study
In-situ Raman
Solid-state NMR spectroscopy

A B S T R A C T

Polymer electrolyte membrane fuel cells (PEMFC) are lagging in commercialization due to the high cost of noble metal catalysts (e.g., Pt) and perfluorosulfonic acid-based (PFSA) membranes. Recycling and reusing these components at the end of life (EoL) could increase the viability and decrease the environmental impact of PEMFCs. In this work, we demonstrate an environmentally friendly method for reprocessing PFSA membranes based on a hydrothermal treatment using only water as a reactant, which is essential for upscaling to an industrial application. In addition, we focused on the recycling process itself and the membrane's recovery as a water-based dispersion, but also investigated the structural, chemical, and mechanical properties and the electrochemical performance of the membranes after being re-cast from the water-based dispersion (denoted as reprocessed membranes). We investigated two different ionomers, a short-side chain (SSC) ionomer with an equivalent weight of 800 (3M-800EW) and a long-side chain (LSC) ionomer with an equivalent weight of 1000 (3M-1000EW), both obtained from 3 M. Both membrane types could be dispersed in water and reprocessed by hydrothermal treatment. No changes in the chemical structure of the ionomers were observed by subsequent IR, Raman, and NMR spectroscopy. However, thermal and mechanical analyses of the reprocessed membranes showed a deterioration of their mechanical properties. The hydrothermal step increased both the water uptake and retention behavior. We attribute this to the expansion of the water channels observed in the SAXS analysis. Full cell tests under standard (80 °C) and harsher (120 °C & 130 °C) operation conditions demonstrated electrochemical performance for the reprocessed 800EW membranes.

## 1. Introduction

Perfluorosulfonic acid ionomers are widely used as solid polymer electrolytes in various electrochemical energy conversion and storage devices, such as polymer electrolyte membrane fuel cells (PEMFCs), PEM water electrolyzers, chlor-alkali electrolyzers and redox flow batteries, because of their excellent mechanical and chemical stability and high proton conductivity [1]. Especially, PEMFCs have become important for future electricity production in the context of "green hydrogen" initiatives. However, the high costs of noble metal catalysts (e.g. Pt) and expensive ionomer production limit the commercialization of these systems. Implementing a recycling route for the components

* Corresponding authorElectrochemical Process Engineering, Universität Bayreuth, Universitätsstraße 30, 95447 Bayreuth, Germany
*E-mail address:* maximilian.kutter@uni-bayreuth.de (M. Kutter).

after their end of life (EoL) can lower the costs and reduce the environmental impact of the precious components [2]. Perfluorinated membranes can cause environmental problems, due to their non-degradable character [3–5]. The recycling and reuse of individual components of PEMFCs after their EoL is not established on a large industrial scale yet. Currently, only a few processes are available, which can neither be implemented on an industrial scale, e.g. due to very complex safety precautions or difficult feasibility in process technology, nor show economic attractivity. In order to make them sustainable, recycling strategies must be developed for the valuable materials used in these energy converters to close the fuel cell resource cycles.

In the last two decades, different approaches have been developed to separate the membranes from the catalyst layers (CLs) and recycle or reuse them. A widely applied method is the separation of the CL from the membrane by organic solvents such as alcohols [6,7]. Shore et al. [8] demonstrated that MEAs can be recycled by separating the catalysts from the membrane in lower alkyl alcohol and alcohol-water solutions and recovering the catalysts by filtration. The PFSA membranes were then dispersed by mild heating of the solution. A similar recycling approach for MEAs from PEM water electrolyzers was reported by Carmo et al. [9] The group treated the MEAs in a home-built reactor using isopropanol and water to separate the catalysts from the membrane. Another approach reported by Grot et al. [10] in 2007 describes the dissolution of the MEA in an autoclave using alcohol-water mixtures, followed by filtration and centrifuging steps to separate the precious metal catalyst from the dissolved ionomer. PFSA membrane recovery is also described by Xu et al. [11] in 2002. After separating the CL and the membrane in an alcohol-water mixture, the membrane was dissolved in dimethyl sulfoxide at 170 °C under atmospheric pressure. Subsequently, new membranes are obtained from the dissolved suspension in a recasting process and evaluated by X-ray diffraction, electrochemical impedance measurements, and polarization curves. Another approach used dimethylformamide as a solvent in an autoclave reaction at 230 °C to dissolve EoL membranes used for redox-flow applications. Afterwards, recycled membranes were processed from the obtained solution and tested for their mechanical strength, water uptake and performance in the battery setup. Interestingly, the group was able to link an increase in water uptake and improved mechanical stability to improved electrochemical performance [12]. However, dimethylformamide poses severe issues with regard to flammability, occupational safety, environmental pollution, and toxicity, thereby lowering its industrial applicability. In 2010, Xu et al. [13] reported an acid-based recycling method, treating the MEA with concentrated sulfuric acid to dissolve the ionomer and separate the catalyst material from the ionomer dispersion by centrifuging. After recasting, the membrane showed slightly lower performance than a pristine membrane. However, the recycling procedure caused the production of $SO_2$ as a side product, which is classified as hazardous and causes environmental problems. Koehler and co-workers [14] developed a solvent-free method to dissolve the membrane and separate the precious metals by a treatment in a supercritical medium (e.g. water). They were able to recover the PFSA ionomer without releasing harmful gases, such as fluorine or hydrogen fluoride, but they did not provide information on the reuse of the PFSA membranes. A detailed investigation of the properties of recycled PFSA membranes was carried out by Sreeraj et al. [4] After CL separation, they analyzed the recovered membranes regarding water uptake, crystallinity, and fuel cell performance. A strategy to dissolve PFSA membranes by hydrothermal treatment using only water as a solvent was first described by Laporta et al. [15] They were able to partially redisperse a long-side chain (LSC) membrane (Nafion-117) and obtained an inhomogeneous gel-like dispersion at temperatures of 250 °C and 280 °C. The recast membranes were studied regarding their water uptake, thermal properties, crystallinity, and proton conductivity. However, they were not tested further for their electrochemical performance in full cell tests and for possible structural changes occurring during their application. In a slightly modified water-based process, we were likewise able to demonstrate that PFSA membranes can be fully dissolved in pure water in a hydrothermal process without the use of organic solvents [16].

Since EoL membranes from fuel cell applications can suffer from equivalent weight (EW) increases and molecular weight (MW) losses, we focused on the reprocessing of pristine (untreated) membranes (not EoL membranes) to better understand whether the recycling process in itself causes degradation phenomena. Therefore, we decided to use the term “reprocessing” instead of “recycling” throughout the text, as “recycling” is the process of converting waste materials into new materials which maintain their original properties [17].

In this work, we report an environmentally friendly, non-toxic potential recycling route for spent PFSA membranes without the use of flammable solvents and their subsequent recovery as homogeneous dispersions and recasting as reprocessed membranes. Two different types of PFSA ionomers, a state of the art short-side chain (SSC) ionomer with an equivalent weight of 800 g mol $^{1}$ (800EW) and a long-side chain (LSC) ionomer with an equivalent weight of 1000 g mol $^{1}$ (1000EW) (Fig. 1), were investigated concerning their morphology and thermal, mechanical, and chemical properties and compared with their corresponding reprocessed counterparts. All pristine and reprocessed membranes were also evaluated in single fuel cell tests at standard and low relative humidity conditions and temperatures up to 130 °C and demonstrated suitable performance.

## 2. Experimental

Information regarding materials, chemicals, and the titration method for IEC determination can be found in the supporting information.

### 2.1. Membrane preparation

The 800EW membranes were prepared by suspending the PFSA (0.5 g) in a propanol/water solution (4.5 g) (95/5 w/w), stirring for 24 h. The slurry was poured onto a Kapton-coated plate and squeegeed with a Coatmaster 509 MC (ERICHSEN GmbH & Co. KG). The membranes were then dried at 80 °C for 30 min, followed by a final annealing step at 180 °C for 10 min. After the thermal annealing step, the membranes were washed and protonated. The membranes were first soaked in a 3 % $H_2O_2$ solution for 1 h, then placed in a fresh Milli-Q water bath for 15 min (at least three times) to wash out the hydrogen peroxide residues. For the protonation step, the membranes were soaked in a 1.5 M $H_2SO_4$ solution for 1 h and washed again in a Milli-Q water bath. The 1000EW membranes were prepared according to the same protocol using an ethanol/water mixture (60/40 w/w).

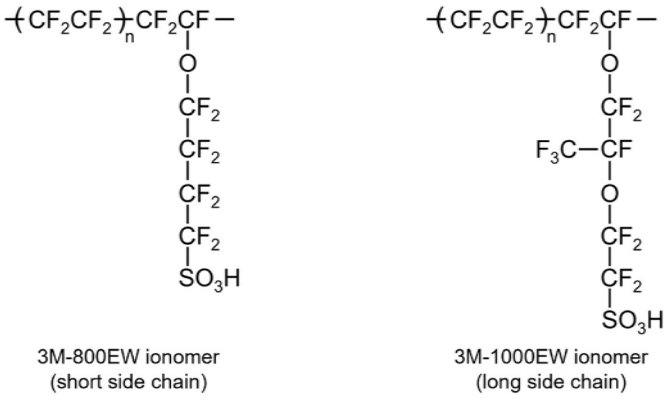


**Fig. 1.** 3 M Perfluorosulfonic acid (PFSA) ionomer structures: 3M-800EW ionomer (SSC) (left) and 3M-1000EW ionomer (LSC) (right).

### 2.2. Hydrothermal process

For reprocessing, 2–5 g of the pristine membranes (Section 2.1) were cut in small pieces and placed in a 125 ml PTFE cup. 42 ml of Milli-Q water was added to the membrane pieces and the cup was placed in a Parr instruments pressure vessel (model 4748). The vessel was sealed and placed in a Memmert UNB 300 oven for 3 h at 230 °C. After the temperature treatment the vessel was allowed to cool down to room temperature. The obtained homogeneous PFSA dispersion was either analyzed as received or dried and used to produce reprocessed membranes.

### 2.3. Reprocessed membrane preparation

The reprocessed membranes were prepared according to the same procedure explained in 2.1, resulting in uniform membranes in the acid form. In comparison to the pristine membranes, their transparency and surface structure appear the same. Photographs of the pristine and reprocessed membranes are shown in Figs. S1 and S2.

### 2.4. Fourier-transform infrared spectroscopy (FTIR)

Infrared spectroscopy measurements were performed using a Bruker Vertex 70 FTIR-ATR spectrometer with a DTGS detector (RT DLaTGS) and a diamond ATR accessory. Spectra were acquired by accumulating 16 scans from 400 to 4000 $cm^{-1}$ at room temperature (spectral resolution: 1 $cm^{-1}$).

### 2.5. Small angle X-ray scattering (SAXS)

Small angle X-ray scattering measurements were performed using a Xeuss 3.0 (Xenocs, France) equipped with a copper source ($\lambda = 1.5418$ Å). Scattering images were detected on an Eiger2 R 1 M detector (Dectris, Switzerland) with 1028 × 1062 pixels and a pixel size of 75 μm × 75 μm located 0.3 m from the sample (deducted via AgBeh calibration). The beam size was adjusted to 0.5 mm × 0.5 mm, and each sample was measured for 2 h in an ambient atmosphere, with single-image exposure times of 30 min. The measured single SAXS images were averaged, 1D cuts extracted, and background corrected for air scattering. Peak positions were determined by fitting each peak profile with a local background and a Gaussian function using XSACT 2.0 (Xenocs, France).

### 2.6. Solid-state nuclear magnetic resonance spectroscopy (ss-NMR)

All $^{13}C$ cross polarization magic-angle-spinning (CP MAS) NMR spectroscopic experiments were performed with a Bruker Avance-III HD spectrometer operating at a $B_0$ field of 14.1 T. The $^{13}C$ ($\nu_0 = 150.9$ MHz) MAS NMR spectra were obtained with a ramped $^{13}C\{^{19}F\}$ CP experiment using a commercial 1.3 mm triple resonance probe (Bruker). The spectra were recorded with a spinning frequency of 60 kHz and a contact time of 1.2 ms. The corresponding nutation frequency $\nu_{nut}$ for the $^{13}C$ channel was set to 40 kHz while the power for the shaped pulse on the $^{19}F$ channel was adjusted to maximal polarization transfer. Fluorine broadband decoupling with a spinal-64 sequence ($\nu_{nut}$ ($^{19}F$) = 12 kHz) was applied during acquisition. For $^{1}H$ ($\nu_0 = 600.1$ MHz) and $^{19}F$ ($\nu_0 = 564.7$ MHz) single-pulse experiments were performed with recycle delays of 3 s and 4 s, respectively. All $^{13}C$ and $^{1}H$ NMR spectra were referenced to tetramethylsilane (TMS) using the secondary standard adamantane while the $^{19}F$ spectra were referenced to trichlorofluoromethane using the secondary standard ammonium perfluorooctanoate.

### 2.7. Thermogravimetric analysis (TGA)

Thermogravimetric analysis (TGA) was performed on a Netzsch STA 449C at a heating rate of 5 K $min^{-1}$ up to 650 °C in a nitrogen atmosphere. Netzsch's Proteus software was used for data evaluation.

### 2.8. Dynamic mechanical analysis (DMA)

Dynamic mechanical analysis (DMA) was conducted on an MCR 702e MultiDrive dynamic mechanical analyzer from Anton Paar. The membranes were cut into rectangular pieces with an area of 14 mm × 8 mm and tested in displacement control mode at a fixed frequency of 1 Hz and an amplitude of 10 μm. The temperature was increased with a constant temperature ramp of 3 K $min^{-1}$ from room temperature up to 135 °C. The tan(δ) values were calculated from the obtained data as a function of temperature.

### 2.9. Water uptake (WU)

Water uptake (WU) from the liquid phase was measured by a gravimetric method using a ABT 220-5DM precision balance (Kern, Germany). Before testing, the samples were dried at 60 °C for 2 h in a drying cabinet to determine the dry mass ($m_{dry}$). Afterwards the samples were immersed in Milli-Q water for 1 h at 25 °C and the surface dried with Kimtech papers. Immediately afterwards, the weight was determined ($m_{wet}$). This procedure was repeated five times and an average value was calculated. Each membrane type was tested at least 3 times. Total water uptake was determined by Equation (1). The water content as a function of water activity ($\lambda_{WU}$) was calculated using Equation (2).

$$WU = \frac{m_{wet} \quad m_{dry}}{m_{dry}} \bullet 100\% \tag{1}$$

$$\lambda_{WU} = \frac{m_{wet} \quad m_{dry}}{m_{dry}} \bullet \frac{EW}{M(H_2O)} \tag{2}$$

### 2.10. Dynamic vapor sorption (DVS)

Dynamic vapor sorption (DVS) measurements were performed using a TA Instruments Q5000 Sorption Analyzer (accuracy ± 0.01 %). Prior to each measurement, the membranes were dried at 80 °C for 2 h and followed by a second drying step at 60 °C for 300 min, which was included in the measurement protocol. After the drying steps, sorption and desorption isotherms were performed at 25 °C by applying relative humidity (RH) steps between 0 % and 90 % RH at 10 % intervals with a ramp rate of 0.5 % $min^{-1}$. Relative humidity values from 0 to 50 % were maintained for 60 min, 60 % RH for 100 min, 70 % and 80 % RH for 120 min, and 90 % RH for 180 min to ensure equilibrium at each RH step.

### 2.11. In-situ Raman spectroscopy

A WITec alpha 300 RA confocal Raman microscope (WITec, Germany) was used to acquire the Raman spectroscopic data. The excitation source was a 40 mW laser operating at a wavelength of 532 nm. A specially designed home-built sample container was employed for in-situ measurements in water immersion. The signal was gathered by the Zeiss W Plan-Apochromat 63×/1.0 objective and a WITec UHTS 300 VIS spectrometer. The spectrometer consists of a 600-groove optical grating, and a Peltier-cooled back-illuminated EMCCD camera with 1600 pixels. Before the Raman measurements, the membranes were submerged in deionized water for at least 1 h to achieve the required hydration level.

A single Raman spectrum was obtained by combining five spectra with an acquisition time of 5 s each. For confocal through-plane scanning, the integration time was set to 20 ms per point with an axial step size of 1 μm. The raw spectra were processed by subtracting the signal background using the software WITec Project FIVE+. A shape-based algorithm was applied, with a noise factor 1 and a shape size 400. Subsequent data processing procedures were performed using MATLAB (MathWorks, USA).

The membranes' equivalent weight (EW) was determined using a calibration curve that was unique to the device. In brief, by obtaining the Raman spectra of the 3 M ionomer for four specific EWs (670, 725, 800, and 980 g mol $^{-1}$), the calibration for the EW was determined and used to quantify the equivalent weight of a 3 M ionomer sample. Details of the method are described elsewhere [18].

The $\nu_s$(O–H) peak (3000–3700 cm $^{-1}$) was taken as a measure for the local water content within a membrane. Integrating the $\nu_s$(O–H) band over the focus position of the through-plane scan yields the spatially resolved water content of the membrane. Earlier, Peng et al. [19] disclosed the details of this approach. The Raman signal of water is not equal above and below the membrane due to the absorption and scattering of light within the membrane. Therefore, the intensity profile was equilibrated to comparable levels by fitting a linear corrective function to the through-plane data. The water volume fraction $\Phi_V$ equals the ratio of the spectral intensities of the $\nu_s$(O–H) peak within the membrane and pure water [19]:

$$\Phi_V = \frac{\rho_{sorbed}}{\rho_{pure}} = \frac{N_{sorbed}}{N_{pure}} = \frac{S_{sorbed}}{S_{pure}} \quad (3)$$

with $\rho$ as the density (g m $^{-3}$) of either sorbed or pure water, N as the number of molecules in the focal spot, and S as the integrated Raman intensity of the $\nu_s$(O–H) band, either sorbed in the membrane or pure water.

### 2.12. Proton conductivity measurements

The ionic conductivity measurements of the membranes were performed in a home-built measurement chamber under controlled PEM conditions (temperature & humidity) using impedance spectroscopy. The setup was based on a commercially available BekkTech cell using the in-plane conductivity measurement mode [20]. Prior to testing, the membranes were cut into pieces of 1 × 2 cm. Depending on the measurement environment, the setup was placed in a beaker filled with water or performed at a constant dew point of 70 °C in a temperature range of 70 °C–130 °C with an equilibration time of 2.5 h for each temperature step. The experiments were controlled by a Hewlett Packard HP 4284A LCR meter at an analysing frequency of 1 MHz–20 Hz with an amplitude of 20 mV.

### 2.13. Fabrication of membrane electrode assembly (MEA)

Membrane electrode assemblies (MEAs) were fabricated using catalyst-coated membranes (CCMs) with an active area of 9 cm$^2$. The electrodes were supplied by 3 M and consisted of an 825 g mol $^{-1}$ ionomer binder, a carbon support with a catalyst loading of 0.1 $mg_{Pt}$ cm $^{-2}$ and 0.2 $mg_{Ru}$ cm $^{-2}$ on the anode side and 0.4 $mg_{Pt}$ cm $^{-2}$ on the cathode side. The electrodes were laminated to the membranes by hot pressing at 180 °C, 0.4 MPa for 60 s. SIGRACET® type 10 AA gas diffusion layers were attached to the MEA. PTFE served as a gas-tight sealing.

### 2.14. Full cell tests

Low-temperature (LT) and intermediate-temperature (IT) PEMFC tests were performed on a Horiba-FuelCon Evaluator-C50-LT in an in-house built single cell with an active cell area of 9 cm$^2$ at three different temperatures (80 °C, 120 °C, and 130 °C). The gas was supplied in counterflow mode. Control and regulation of the media supply and monitoring of the cells were performed using the Testwork software. All cell tests were carried out in hydrogen-air mode.

For the break-in procedure, the cell was heated to 45 °C. The gases were set to 85 °C and 20 % RH with constant flow rates of 0.5 l min $^{-1}$ on the anode and 1.5 l min $^{-1}$ on the cathode side. After the cell reached a steady state, a constant current of 0.11 A cm $^{-2}$ was applied for 3 h. Afterwards, the cell temperature was increased to 80 °C with 20 % RH and three galvanostatic polarization curves were recorded with increasing current steps (Table S4), each hold for 2 min, from OCV to a potential limit of 0.2 V. After the conditioning steps, three galvanostatic polarization curves were recorded for each operating condition (Tables S5–S7). All membranes were characterized by parameters obtained using a harmonized testing protocol for automotive applications from the European Commission [21].

## 3. Results and discussion

In this work, a strategy for PFSA membrane recycling is presented for which two different ionomers were selected, one with a short side chain (3M-800EW) and one with a long side chain (3M-1000EW). The pristine and reprocessed membranes were analyzed for their structural, mechanical, and electrochemical properties.

### 3.1. Characterization of the reprocessed membranes

**EW/IEC** – The equivalent weights have been calculated using Raman spectroscopy and titration, to evaluate the changes in the ionomer during the hydrothermal process. The values for the four membranes are shown in Table 1. For the 800EW membranes the analyses yielded EWs of 831 ± 15 g mol $^{-1}$ and 824 ± 7 g mol $^{-1}$ for the pristine membrane and 833 ± 15 g mol $^{-1}$ and 830 ± 7 g mol $^{-1}$ for the reprocessed membrane. The EW values for the 1000EW membranes investigated by Raman spectroscopy do not show any change in chemical properties yielding EWs of 852 ± 15 g mol $^{-1}$ before and 854 ± 15 g mol $^{-1}$ after the hydrothermal process. The titration method shows however slightly higher values of 890 ± 7 g mol $^{-1}$ and 883 ± 7 g mol $^{-1}$, respectively. Thus, we cannot observe any change in the EWs by the hydrothermal process of the SSC and the LSC ionomer within the error margin of the applied methods. The reason for the comparatively large difference between the measured and theoretical EWs for the LSC ionomer could not be identified in our experiments, but will be followed up with. The ion exchange capacity (IEC) was calculated using the EW values from titration (see SI for experimental details).

**Thermo-mechanical analysis (TGA/DMA/Tensile tests)** – PFSA membranes consist of a strong PTFE-based backbone that not only provides mechanical strength and thermal stability but also prevents the membrane from dissolving in water. However, under the hydrothermal process parameters we applied, the membranes can be redissolved in water. Thermo-mechanical analyses, here TGA and DMA analyses, should further prove whether the thermal treatment influenced the stability of the side chain and crystallinity of the backbone (TFE repeat unit). The respective results are shown in Fig. 2. The TGA profiles for all four membranes show the typical degradation behavior for 3 M SSC membranes (a) and Nafion-type LSC membranes (b). In both cases, an initial weight loss can be observed between room temperature and 300 °C, corresponding to bound water (I). The first degradation of the ionomer can be seen at 320–325 °C for the 800EW membranes and at 290–295 °C for the 1000EW membranes, respectively. This degradation can be attributed to the loss of the sulfonic acid group of the side chain

**Table 1**
Membrane thickness, equivalent weight measured by titration and Raman method, ion exchange capacity of the 800EW, the 800EW_re, the 1000EW and the 1000EW_re membrane: *values obtained by Raman method; **values obtained by titration. The ionomer for the 800EW samples and the 1000EW samples were each obtained from a single batch.

| Membrane | Thickness (μm) | *EW (g mol $^{-1}$)* * | *EW (g mol $^{-1}$)* ** | *IEC (mmol g $^{-1}$)* ** |
|---|---|---|---|---|
| 800EW | 35 ± 2 | 831 ± 15 | 824 ± 7 | 1.21 |
| 800EW_re | 32 ± 3 | 833 ± 15 | 830 ± 7 | 1.20 |
| 1000EW | 75 ± 3 | 852 ± 15 | 890 ± 7 | 1.12 |
| 1000EW_re | 72 ± 3 | 854 ± 15 | 883 ± 7 | 1.13 |

(II) [22–24]. The remaining polymer side chain degrades at 380 °C (800EW) and 350 °C (1000EW) (III) followed by the decomposition of the remaining PTFE backbone beyond 440 °C and 420 °C, respectively (IV) [3,22,25]. The thermal stability of the reprocessed membranes is similar to the pristine membranes indicating that the hydrothermal treatment does not have a significant impact on the thermal stability of the reprocessed membranes.

The mechanical and thermal properties of the pristine and reprocessed membranes were tested by DMA and the respective measurements are shown in Fig. 2c and d. The glass transition temperatures ($T_g$) of the pristine 800EW membrane can be observed at 122 °C, which is in good agreement with literature values [26], whereas the $T_g$ of the 800EW_re only reached 115 °C. The loss in $T_g$ indicates a reduced membrane crystallinity and an earlier onset of the segmental movement of the main chain and the interconnected static network of the fluorocarbon matrix, which is due to the hydrothermal treatment.

Tensile tests were carried out to investigate the stiffness of the membranes before and after hydrothermal treatment. The stress-strain curves are shown in Fig. S3. The Young's modulus of the 800EW membranes decreases from 110 MPa (800EW) to 77 MPa (800EW_re) due to the treatment, while the elongation to break for the 800EW_re is 60 %. A similar result is observed for the 1000EW LSC membranes shown in Fig. S3b (note: in this case the elongation to break value could not be reached due to experimental test protocol). Tensile test results show a lower stiffness for the reprocessed material, similar to the SSC ionomer. The Young's modulus (E) decreases from 107 MPa (1000EW) to 83 MPa (1000EW_re). Corresponding data obtained from the stress-strain curves are shown in Table S1. The observed lower modulus of the reprocessed membranes could be an indication of lower molecular weights (MW) as shown by Gittleman et al. [27].

**Vibrational spectroscopy (IR/Raman)** – Vibrational spectroscopy of the pristine and reprocessed membranes was conducted to analyze changes in the chemical composition, like the cleavage of the side chain, due to the hydrothermal process. The IR spectra of the 800EW and the 800EW_re are shown in Fig. 3a. Both 800EW membranes show the expected backbone-related bonds $\nu_a(C–F)_{bb}$ and $\nu_s(C–F)_{bb}$ at 1196 cm $^{1}$ and 1142 cm $^{1}$, respectively [28]. The 1055 cm $^{1}$ and 989 cm $^{1}$ peaks can be associated with the symmetric stretching of the sulfonic acid group $\nu_s(S–O)_{sc}$ and the $\nu_s(C–O–C)$ bond connecting the backbone and side chain [29,30]. The $\nu_s(C–C)$ band can be found at 1342 cm $^{1}$ [31]. The IR measurements of the 1000EW ionomers, seen in Fig. 3b, indicate that the hydrothermal process does not change the chemical structure of the membranes [28]. The two most prominent bands at 1199 cm $^{1}$ and 1138 cm $^{1}$ can be assigned to the backbone's $\nu_a(C–F)_{bb}$ and $\nu_s(C–F)_{bb}$ bonds [30]. Here, the side chain-related bond at 970 cm $^{1}$ is more pronounced due to the higher amount of $\nu_s(C–O–C)$ bonds in the long side chain ionomer (Fig. 1). According to the literature the peak at 1311 cm $^{1}$ has been associated with the $\nu_a(CF_3)_{sc}$ vibration and the band at 1055 cm $^{1}$ with the $\nu_s(S–O)_{sc}$ bond [29].

After comparing the differences between the Raman spectra of Nafion, 3 M ionomer, and Aquivion, Maier et al. [18] were able to examine the ionomer's distinctive bonding. Therefore, we assign the peak at 730 cm $^{1}$ to the symmetric stretching $\nu_s(C–F)_{bb}$ of the PTFE backbone. The side chain-related bands at 711 cm $^{1}$, 768 cm $^{1}$, 1017 cm $^{1}$, and 1061 cm $^{1}$ are attributed to the $\nu_s(C–S)$ stretching, the $\nu_s(C–F)_{sc}$ band of the C–F bonds in the side chain, the $\nu_s(C–O–C)$, and the $\nu_s(S–O)$ vibration, respectively. For all backbone and side chain associated modes, the Raman spectra of the reprocessed and pristine membranes are equal in spectral intensity and location for the 800EW and the 1000EW 3 M ionomer and do not change for the reprocessed membranes.

**MAS NMR spectroscopic-analysis** – Additional to vibrational spectroscopy, high-resolution solid-state NMR spectroscopy was applied to analyze potential structural changes of the ionomers upon reprocessing. The $^{19}F$ spectra of the 3M-800EW (SSC) and 3M-1000EW (LSC) ionomers are given in Fig. 4 and are normalized to the prominent $CF_2$

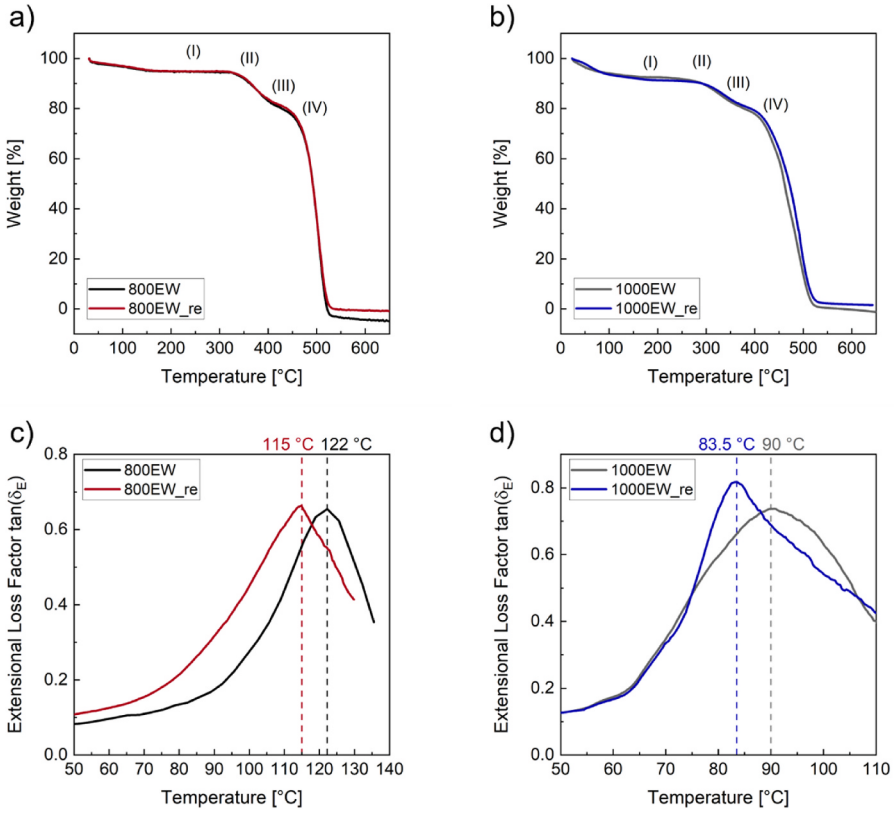


**Fig. 2.** TGA profiles of 800EW and 800EW_re membranes (a) and 1000EW and 1000EW_re membranes (b), and temperature-dependent tan(δ) of the 800EW and 800EW_re membranes (c) and 1000EW and 1000EW_re membranes (d) measured by DMA.

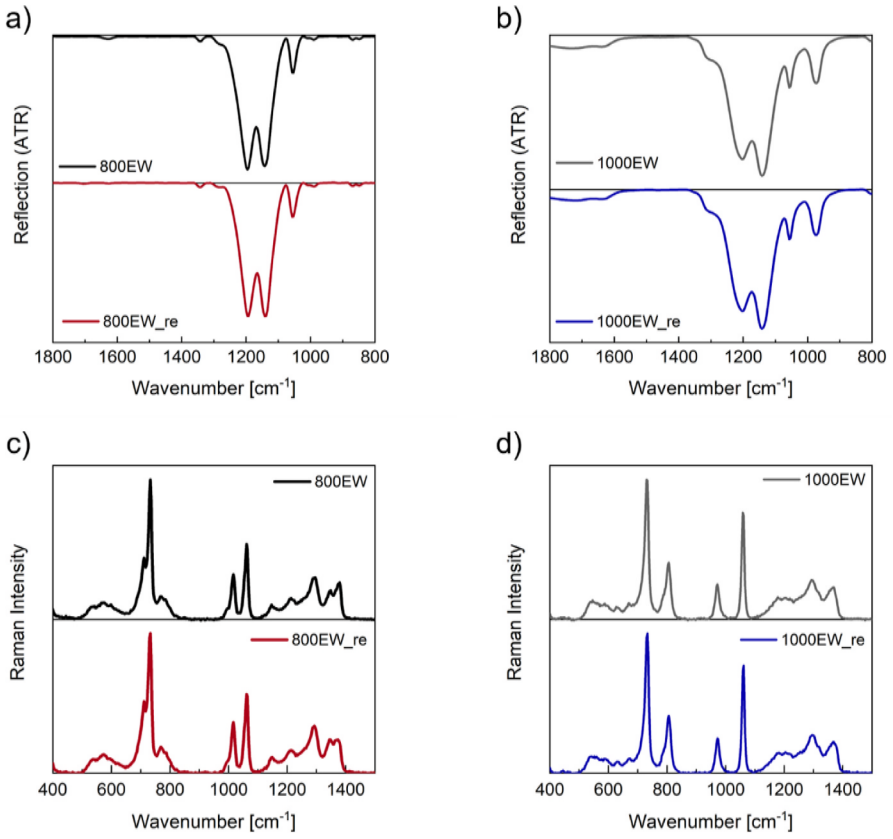


**Fig. 3.** IR spectra of the 800EW and 800EW_re membranes (a) and the 1000EW and 1000EW_re membranes (b). Raman spectra of the 800EW and 800EW_re membranes (c) and the 1000EW and 1000EW_re membranes (d). The IR and Raman spectra are normalized to the prominent $CF_2$ backbone peak at 1138 $cm^{-1}$ and 730 $cm^{-1}$, respectively. Superimposed spectra are shown in Fig. S4 & Fig. S5.

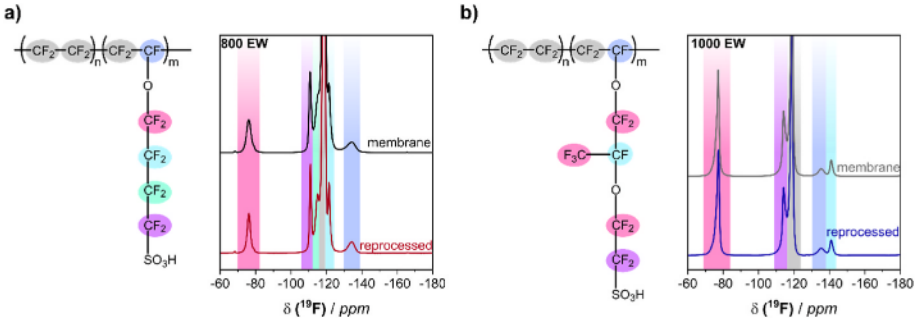


**Fig. 4.** $^{19}F$ MAS NMR spectra of the 800EW (a) and 1000EW (b) pristine and reprocessed membranes, all with color-coded signal assignment according to Ghassemzadeh et al. [32] [[,33] [][][], Chen et al. [34] and Robert et al. [35] The spectra are normalized to the prominent $CF_2$ backbone resonances. The corresponding $^{13}C\{^{19}F\}$ CP MAS NMR spectra are shown in Fig. S6, while the superimposed $^{19}F$ MAS NMR spectra are shown in Fig. S7. (For interpretation of the references to color in this figure legend, the reader is referred to the Web version of this article.)

backbone resonances ( 119 ppm). For the SSC ionomer (Fig. 4a) five additional signals are visible, which are assigned to the four sidechain $CF_2$ groups ( 76 ppm, 121 ppm, 115 ppm, and 111 ppm with increasing distance to the ether group) and to the backbone CF group ( 134 ppm). In the spectra of the LSC ionomer (Fig. 4b), the signals at 135 ppm and 141 ppm are attributed to the backbone and sidechain CF groups, respectively, while the signal at 114 ppm corresponds to the $CF_2$ group next to the sulfonic acid residue. The O-$CF_2$ and $CF_3$ groups give rise to a superimposed resonance at 77 ppm. The spectral assignments are based on previous work from Ghassemzadeh et al. [32, 33] on SSC ionomers (Hyflon Ion) and earlier work by Chen et al. [34] and Robert et al. [35] on LSC ionomers (Nafion). The chemical shifts and intensity ratios of the $^{19}F$ NMR resonances for the pristine and reprocessed membranes are similar (values can be found in Table S2). Sharper resonances are observed for the reprocessed membranes indicating increased local mobility due to decreased membrane crystallinity. Similar observations are made in the respective $^{13}C$ CP MAS spectra (Fig. S6). The similarity of the spectra of pristine and reprocessed membranes indicates the absence of structural changes during the hydrothermal process. This result is in good agreement with the IR and Raman data.

**Water uptake** –Three different techniques have been used to determine the WU of the pristine and reprocessed membranes from vapor as well as liquid water. The WU was analyzed by gravimetrically determined WU, in-situ Raman measurements and dynamic vapor sorption providing a rather complete picture of the interaction of water

with the membranes also trying to mimic the situation during realistic operation conditions. The complementarity of the techniques surely helps to obtain a detailed insight into the water-membrane interaction. The total water uptake of the pristine and the reprocessed membranes can be seen in Figs. S8a and S8b. The water uptake of the 800EW membrane is at 38 % of its initial weight, whereas the reprocessed membrane's water uptake increases by around 4 %. This observation corresponds to a water activity (λ) of 16 and 22, respectively. The value for the 800EW is in good agreement with the literature values [36]. For the 1000EW membranes the differences between the pristine and the reprocessed membrane increased dramatically due to the hydrothermal process. The pristine membrane showed a WU of 31 %, while WU of the reprocessed 1000EW membrane increased by 18 % to a total water uptake of 49 %. The corresponding λ values are 14 and 24.

The water uptake was quantified in-situ and spatially resolved with confocal Raman microscopy. In this measurement, the quantity representing the water uptake of PFSA membranes is the water volume fraction, which was evaluated with confocal through-plane scans in water immersion (Equation (3)). The 800EW and 1000EW 3 M ionomers show a uniform water volume fraction over focus depth for the pristine and reprocessed membranes (Fig. 5a and b). 800EW pristine and reprocessed membranes exhibit the same water volume fraction of 56 %, corresponding to a hydration number of $\lambda = 29$ $[H_2O]/[SO_3H]$, for both membranes. The similar water volume fractions indicate only a slight increase in water uptake of the membranes after the hydrothermal process. In contrast, the water volume fraction for the 1000EW membranes increases from 49 % ($\lambda = 23$) to 56 % ($\lambda = 30$) after subjecting the membrane to the hydrothermal process. This underlines that the water uptake rises substantially for the recast membranes due to the reprocessing step, at least for the 1000EW. The increased water uptake of the reprocessed membranes is directly correlated to the reduced modulus (described in the *Thermo-mechanical analysis* section). A lower modulus indicates less ionic chain cross-linking and therefore greater side chain mobility, resulting in a lower glass transition temperature and swelling resistance [37]. The measurements of the water volume fraction and the hydration numbers confirm the measurements of the total water uptake and follow the same trend.

The dynamic water sorption was additionally measured to evaluate the water uptake from water vapor at different RH, which is closest to the fuel cell operating conditions. The water vapor sorption measurements in Fig. 5, reveal a slight increase in water uptake, comparing the pristine with the reprocessed samples. The differences are marginal, with an increase of 1 % for the 800EW or 4 % for the 1000EW membrane at 90 % RH (Fig. 5c and d). Similar results have been obtained by Onishi et al. [38] and Kusoglu et al. [39] investigating a pre-dried (as-received/pristine) and pre-boiled (saturated in boiling water) membrane. They found that a pre-dried membrane takes up a similar amount of water regardless of whether it is saturated with liquid or vapor water. However, a pre-boiled membrane behaves differently; in liquid water the λ-values are much higher than in water vapor. The same behavior can be observed with the pristine and reprocessed membranes. The hydrothermal process applies an extreme form of pre-boiling. Due to the process, the reprocessed membrane is already in quasi-equilibrium and shows a vapor-liquid difference. This observation could be confirmed by temperature-dependent investigations [38] [–] [40], where the liquid water uptake of pre-boiled membranes does not change with temperature [38,39].

The reason for the change between liquid and vapor sorption is not profoundly understood. However, some investigations have been carried out, revealing a change throughout the bulk of the ionomer or at the

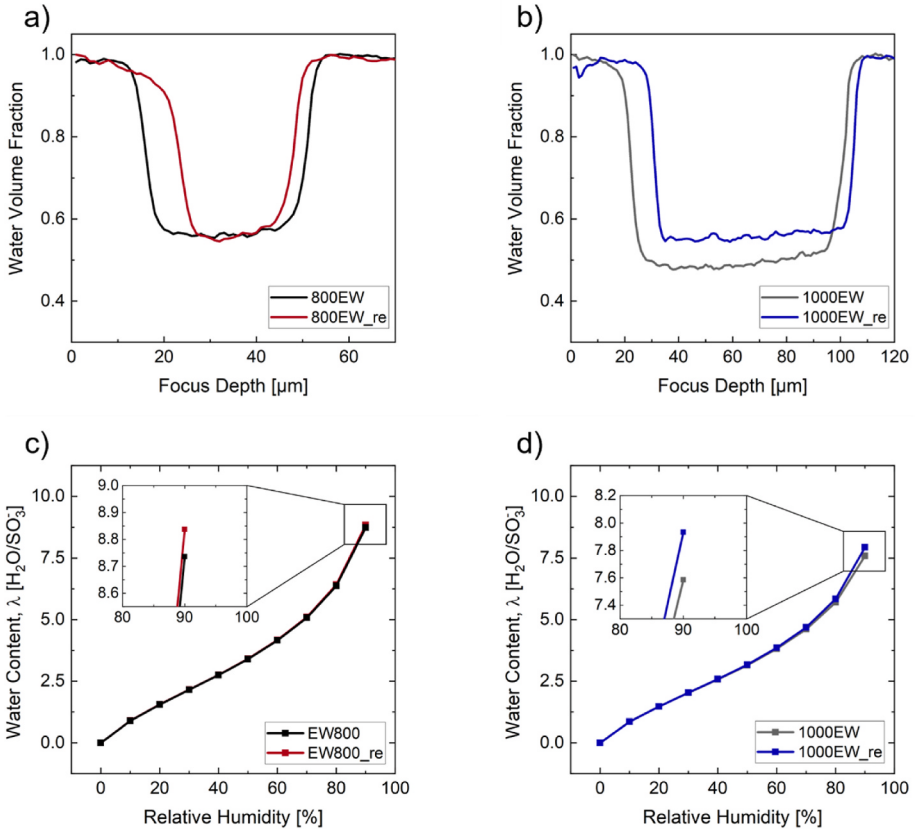


**Fig. 5.** Water volume fraction and water vapor sorption isotherms of pristine and reprocessed membranes. The water volume fraction of the 800EW and 800EW_re membranes (a) and the 1000EW and 1000EW_re membranes (b) were obtained from confocal Raman spectroscopy in water immersion at 25 °C. The water volume fraction was calculated according to Equation (3). The spectral area of the $\nu_s$(O–H) peak was used to determine the Raman signal of pure and sorbed water over the focus depth. Water vapor sorption isotherms of the 800EW and 800EW_re membranes (c) and the 1000EW and 1000EW_re membranes (c) at 25 °C.

interface, e.g. due to the thermal history of the membrane [41,42]. Studies by Kusoglu et al. [39] focused on SAXS investigations to gain structural information on pre-dried and pre-boiled membranes under dry and wet conditions, which served as a basis for our SAXS measurements.

**SAXS** – Small angle X-ray scattering is a powerful tool to study the morphological properties of dry and hydrated PFSA ionomers, and to investigate the effects of temperature, humidity or aging on crystallinity [1]. SAXS measurements can provide information about the microstructure and the phase separation under certain conditions [43]. The primary information from the scattering pattern are the ionomer peak, the matrix knee and the upturn in the low $q$-region. The ionomer peak corresponds to the distance between the hydrophilic domains and the hydrophobic phase and can be associated with water uptake and retention by calculating the distance between individual water channels. The matrix knee, typically observed between $q = 0.04–0.08$ Å $^{-1}$, can provide information about the backbone and the intercrystalline domain spacing [44].

The SAXS curves of the pristine and reprocessed membranes under dry and wet conditions are shown in Fig. 6. The SAXS patterns of the 800EW membranes show the typical ionomer peak at around 0.2 Å $^{-1}$. Comparing both membranes, a slight shift in peak position can be observed from $q = 0.183$ Å $^{-1}$ (pristine) to $q = 0.190$ Å $^{-1}$ (reprocessed). The resulting interphase spacing, the $D$-spacing [43], defined as $2\pi/q$, decreases from 34.3 Å to 33.1 Å, indicating smaller channel diameters for the reprocessed 800EW membrane. After wetting, a shift in the ionomer peak position to smaller $q$-values can be noticed, indicating a larger water-domain spacing. The spacing increased by 6 % for the pristine and 9 % for the reprocessed membrane, respectively. Smaller values are obtained if the channel diameters are calculated using the (parallel) cylindrical model of Schmidt-Rohr and Chen [45]. Under wet conditions, the channel diameters increase from 22.9 Å to 24.2 Å (pristine) and from 22.1 Å to 24.1 Å (reprocessed). This higher expansion rate of the spacing, by 6 % (pristine) and 9 % (reprocessed), might explain the slightly higher WU for the reprocessed membrane seen in the gravimetrically measured WU and the Raman WU studies. These results agree with previous SAXS experiments reporting an increase in water domain distances between pristine and pre-boiled membranes [39,43].

Fig. 6b shows the SAXS patterns of the LSC 1000EW membranes. Here, the ionomer peak at $q > 0.2$ Å $^{-1}$ and the matrix knee are visible. Comparing the ionomer peak of the pristine and the reprocessed membrane, a slight change in peak position can be observed with $q = 0.217$ Å $^{-1}$ and $q = 0.221$ Å $^{-1}$, respectively. In the wet state, the peaks shift to smaller values with $q = 0.206$ Å $^{-1}$ for the pristine and $q = 0.213$ Å $^{-1}$ for the reprocessed LSC membrane, which corresponds to an increase in diameter of 1.5 Å and 1.1 Å for the $D$-spacing, respectively. Comparing the values from the (parallel) cylindrical model [45], the water channels were enlarged by 1.0 Å and 0.7 Å (values can be found in Table S3). Considering the SAXS measurements, the strong water absorption observed for the 1000EW reprocessed membrane is probably not caused by a significant increase in the water-domain spacing. However, it is noticeable that the hydrothermal process has changed the position of the matrix knee. The peak shifted to larger $q$-values after the process. This shift indicates changes in the crystalline domain, which have already been reported for preboiled membranes [39]. Pre-boiling of membranes disturbs the crystalline order, observed by a lower intensity of the crystalline peak (matrix knee), which usually increases the water-domain spacing and enhances the water uptake [39,46]. The SAXS results are in good agreement with water uptake measurements from liquid water and DMA measurements showing decreased thermal stability due to the more strongly disordered crystalline backbone.

### 3.2. *Electrochemical characterization*

**Conductivity** – The conductivity of the pristine and the reprocessed membranes was studied under two different conditions. All membranes were tested in their fully hydrated state (water-soaked) at 25 °C (Fig. S9a), whereas the 800EW membranes were additionally measured under LT- and IT-PEM conditions at 70–130 °C and between RHs of 10–90 %. (Fig. S9b). As expected, in the fully hydrated state the SSC ionomer shows an improved conductivity (0.26 S cm $^{-1}$) compared to the LSC membranes (0.13 S cm $^{-1}$). Notably, in the fully hydrated state, the ion conductivity of the 800EW membrane does not change after the hydrothermal process (Fig. S9a), which is consistent with the WU measurements of the SSC membranes. In contrast, the conductivity significantly improved at IT-PEM conditions of low RH and temperatures around 130 °C, from 4.16 mS cm $^{-1}$ to 6.87 mS cm $^{-1}$ (Fig. S9b).

The 1000EW membrane, however, showed a considerable improvement in conductivity under full hydration (Fig. S9a). After the hydrothermal process, the conductivity increased from 0.13 mS cm $^{-1}$ to 0.20 mS cm $^{-1}$, which can be explained by the higher water absorption of the LSC membrane (gravimetrically determined WU, Fig. S8). Similar results have been obtained and shown in an earlier study by Laporta et al. [15].

**Fuel cell performance** – The fuel cell performance of the membranes was measured by recording polarization curves at various operating conditions (Fig. 7), focusing on moderate and especially dry conditions in $H_2$-air mode. Polarization curves should provide an indication of the membrane's general applicability, while their durability should rather be accessed by long-term OCV and controlled accelerated stress tests (not yet done). At 80 °C and 20 % RH, the pristine 800EW membrane shows a lower PPD with 92 mW cm $^{-2}$ compared to 117 mW cm $^{-2}$ for the reprocessed one. Increasing the RH at LT-PEM conditions, the reprocessed membrane also surpasses the pristine one (Fig. 7b). A

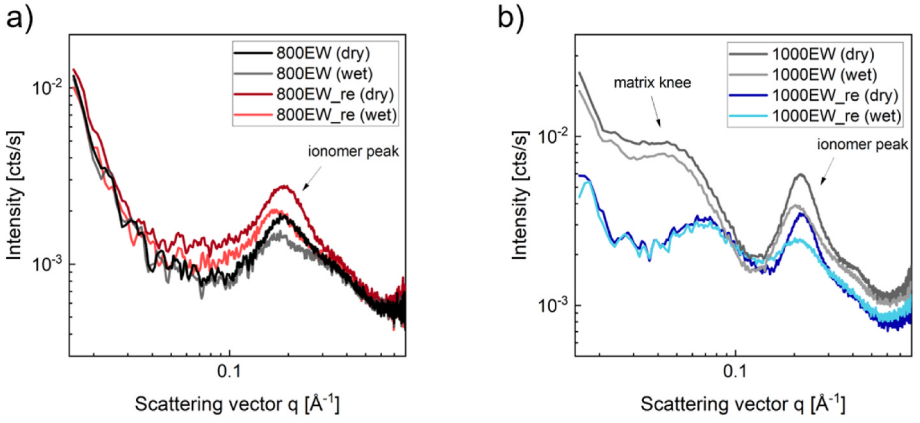


**Fig. 6.** SAXS patterns of the pristine and reprocessed PFSA membranes. (a) SAXS patterns of the 800EW and 800EW_re membranes at 25 °C at 0 % RH and water-soaked. (b) SAXS patterns of the 1000EW and 1000EW_re membranes at 25 °C at 0 % RH and water-soaked.

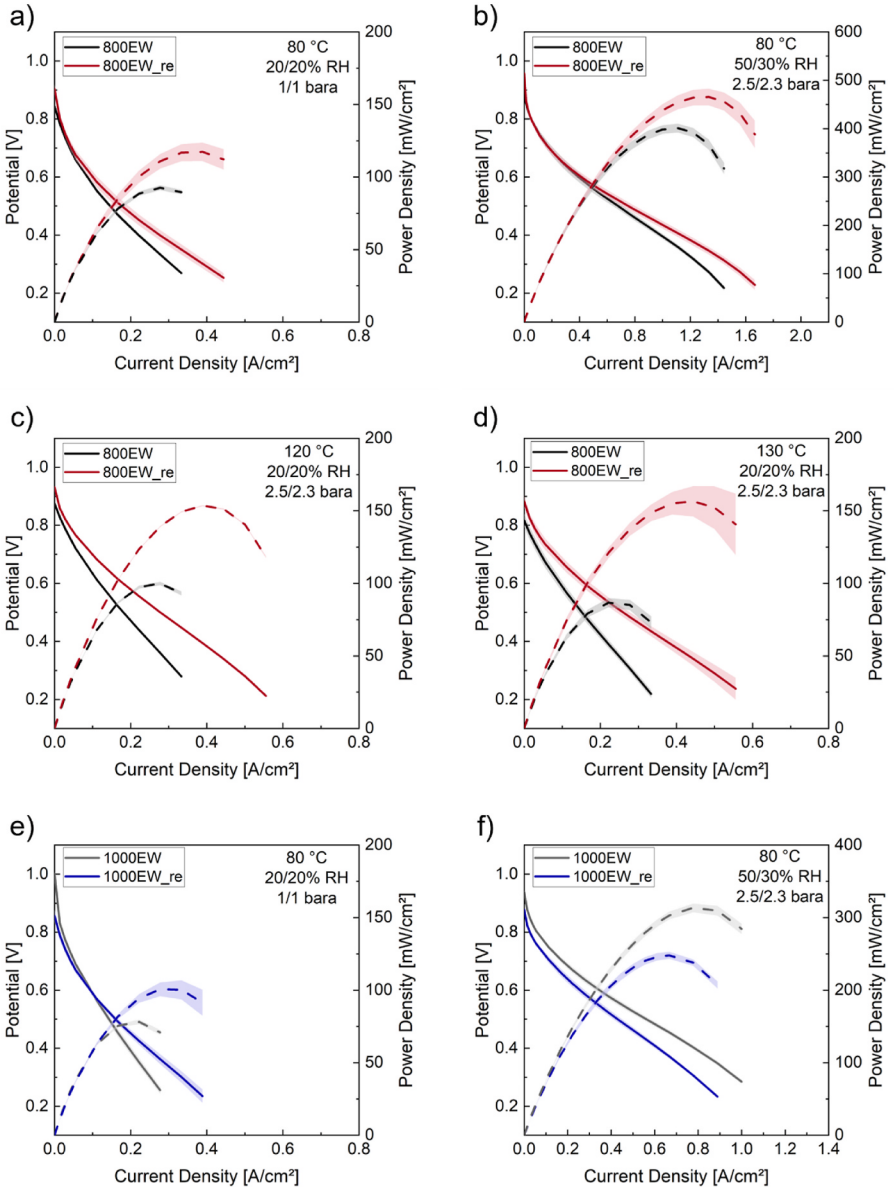


**Fig. 7.** Polarization and power density curves of the pristine and the reprocessed membranes for the 800EW and 800EW_re membranes at 80 °C, 20/20 % RH, 1/1 bara (a); at 80 °C, 50/30 % RH, 2.5/2.3 bara (b); at 120 °C, 20/20 % RH, 2.5/2.3 bara (c); at 130 °C, 20/20 % RH, 2.5/2.3 bara (d); for the 1000EW and 1000EW_re membranes at 80 °C, 20/20 % RH, 1/1 bara (e); at 80 °C, 50/30 % RH, 2.5/2.3 bara (f). Each curve represents the mean of at least three replicate measurements with the respective standard deviations indicated by the shaded areas.

PPD of 466 mW cm $^{2}$ can be observed after the hydrothermal treatment, corresponding to an increase of 65 mW cm $^{2}$. The FC results do not correspond with expectations seen in the gaseous phase's water uptake, but rather follow the trend shown in the conductivity measurements at low RHs.

Fig. 7c and d compare the membranes at IT-PEM conditions, i. e. higher temperatures and low RH. Here, the performance of the reprocessed membranes also increased. At cell temperatures of 120 °C, the PPD increased from 100 mW cm $^{2}$ (800EW) to 154 mW cm $^{2}$ (800EW_re), which was unexpected as the glass transition temperatures (Fig. 2c) dropped below the operating cell temperatures. This should lead to reduced membrane crystallinity and ionomer network stability, resulting in reduced membrane stability together with reduced cell performance [47]. Even at cell temperatures of 130 °C, which is 15 °C above the glass transition temperature of the reprocessed 800EW membrane and the 800EW ionomer [26], the PPD of the reprocessed membrane remained around 150 mW cm $^{2}$, compared to 87 mW cm $^{2}$ for the pristine membrane. However, this does not take into account the annealing step, which the membranes have been subjected to, when linking electrode and membrane in a short hot-press step (see experimental). Following the same trend as the conductivity measurements, we assume that water retention is enhanced for the reprocessed membrane, leading to the observed increased PPDs at IT-PEM temperatures.

The results for the 1000EW membranes are shown in Fig. 7e and f. Due to the lower glass transition temperature of the LSC ionomer, these samples were only tested at 80 °C. Under lower RH (Fig. 7e), the reprocessed membrane reached a higher PPD compared to the pristine membrane (100 mW cm $^{2}$ vs. 78 mW cm $^{2}$). Since the low RH performance of SSC ionomers was expected to be superior compared to LSC ionomers, lower performances were expected due to more substantial dehydration of the membrane resulting in a decrease in proton conductivity [48]. However, after the hydrothermal treatment, the LSC ionomer matches the performance of the pristine 800EW ionomer. Comparing the LSC membranes at higher RH (Fig. 7f) the performance

of the pristine membrane was higher than for the reprocessed membrane. The pristine sample reached a PPD of 313 mW cm $^{2}$, whereas the reprocessed membrane reached only ~250 mW cm $^{2}$.

Worth noting here are, however, the low OCV values under harsh conditions (particularly in Fig. 7d and e). We assume that the low values are due to increased hydrogen crossover during the test runs, either because the high temperatures led to rapid pinhole formation or because the low RH caused poor membrane sealing in the cell setup. Furthermore, it must be considered that polarization curves always reflect the overall behavior of the full cell and do not allow for the precise determination of individual contributions, e. g. from the membrane, the electrodes or even other factors. Further investigations, such as electrochemical impedance spectroscopy (EIS) with coupled DRT analysis or high-frequency resistance (HFR) measurements in combination with OCV hold tests, would be necessary to determine the individual membrane contribution and its degradation properties under cell conditions. Nevertheless, it is remarkable that the reprocessed membranes perform well, even under harsh operating conditions.

In general, the hydrothermal process can increase the FC performance for SSC and LSC ionomers at moderate and harsh cell conditions, shown by proton conductivity and full cell testing. The higher performance can be correlated to an interplay between water uptake and water retention, caused by changes in the microenvironment of the fluorocarbon matrix.

## 4. Conclusion and outlook

In this article, we reported an economically attractive and environmentally friendly potential recycling route for SSC and LSC PFSA membranes, based on a hydrothermal treatment only using water as the solvent. We combined the recovery and recasting of membranes from the obtained homogenous dispersions with their detailed chemical, mechanical, and electrochemical study.

The proposed hydrothermal process did not change the equivalent weight/ion exchange capacity, underlining that no significant degradation of the sulfonic acid group occurred. These results could be further corroborated by spectroscopic analyses, such as IR, Raman, and solid-state NMR spectroscopy showing no side chain cleavages or backbone degradation. The treatment further seemed to increase water uptake from liquid and vapor water, resulting in an enhanced proton conductivity and higher power density values at LT- and IT-PEMFC conditions for the 800EW ionomer. The reprocessed 1000EW ionomer showed an increased peak power density at 80 °C and low RH (20 %), but a slightly decreased peak power density at higher RH (50 %/30 %). SAXS measurements under dry and wet conditions further revealed that the higher water uptake originated from an expansion of the water channels and the disordering of the crystalline domains, similar to structural changes reported for pre-boiled membranes. Complementary DMA and tensile strength measurements showed a decrease in mechanical properties. These, however, were not found detrimental to the fuel cell performance in the first place.

In future work, long-term stability testing by various accelerated stress tests (ASTs), such as OCV hold protocols, should be done in follow-up experiments to study the membrane's degradation behavior and stability further. These studies will help to reveal the structure-performance relationship at realistic operating conditions. In addition, gas permeability measurements should be carried out to analyze the effect of the hydrothermal treatment and the resulting increased water channel dimensions on potential gas crossover. In a further step, the developed process should be tested on aged membranes, either aged by an ex-situ method or, even better, after prolonged use in a PEMFC. These membranes are likely to suffer both equivalent weight (EW) increases and molecular weight (MW) losses at their EoL, which can significantly affect their properties. It is necessary to separate the intact ionomer from the highly degraded polymer fractions. As the degraded ionomer has a lower suspension capacity and therefore a higher EW, a temperature-dependent process might be used for separating the different ionomer fractions.

The herein reported environmentally friendly and industrially scalable recycling method for PFSA membranes could pave the way for low-cost "green hydrogen" production, as it allows recycling of costly components and offers an attractive resource cycle.

## CRediT authorship contribution statement

**Maximilian Kutter:** Conceptualization, Data curation, Formal analysis, Investigation, Methodology, Project administration, Validation, Visualization, Writing – original draft, Writing – review & editing. **Christopher Greve:** Formal analysis, Investigation, Writing – original draft, Writing – review & editing. **Maximilian Maier:** Formal analysis, Investigation, Writing – original draft, Writing – review & editing. **Monja Schilling:** Investigation, Writing – original draft, Writing – review & editing. **Anika Mauel:** Investigation, Visualization, Writing – original draft. **Annika Hilgert:** Investigation, Methodology, Validation, Visualization. **Hendrik Hoffmann:** Investigation. **Wiebke Hagemeier:** Investigation. **Andreas Rosin:** Data curation, Methodology, Writing – review & editing. **Mark Muggli:** Funding acquisition, Resources. **Roswitha Zeis:** Funding acquisition, Supervision, Writing – review & editing. **Jürgen Senker:** Funding acquisition, Supervision. **Thomas Böhm:** Funding acquisition, Supervision, Writing – review & editing. **Eva M. Herzig:** Funding acquisition, Supervision. **Thorsten Gerdes:** Conceptualization, Funding acquisition, Resources, Supervision. **Christina Roth:** Conceptualization, Funding acquisition, Project administration, Resources, Supervision, Writing – review & editing.

## Declaration of competing interest

The authors declare the following financial interests/personal relationships which may be considered as potential competing interests:

Maximilian Kutter, Mark Muggli, Andreas Rosin, Thorsten Gerdes and Christina Roth have patent #Process for Recycling a Solid Article Including a Fluorinated Polymer (WO2023/111750A1) licensed to 3 M Innovative Properties Company.

## Data availability

Data will be made available on request.

## Acknowledgments

Financial support from the Bavarian Ministry of Economic Affairs, Regional Development and Energy (StMWi) under the project "HyRunCell" is gratefully acknowledged. Monja Schilling gratefully acknowledges financial support through a Kekulé Ph.D. fellowship by the Fonds der Chemischen Industrie (FCI). This work contributes to the research performed at CELEST (Center for Electrochemical Energy Storage Ulm-Karlsruhe). Christopher Greve and Eva M. Herzig acknowledge funding from "Bayerisches Staatsministerium für Wissenschaft und Kunst" for funding under Solar Technologies go Hybrid (SolTech). This work made use of DFG (INST 91/443-1). Maximilian Kutter, Christina Roth, Eva M. Herzig, Anika Mauel and Jürgen Senker and gratefully acknowledge the financial support provided by CRC 1585 (PrNo 492723217). In addition, Anika Mauel and Jürgen Senker would like to thank the DFG for financial support within the framework of CRC 1357 (PrNo 391977956). We thank Dr. Florian Mack from Freudenberg e-Power Systems for the fruitful discussions and support during the fuel cell tests. The authors thank Ute Kuhn for supporting and carrying out the dynamic mechanical analyses and the tensile tests at the Department of Polymer Engineering at the University of Bayreuth. We also like to thank Angelika Kreis (Electrochemical Process Engineering – University of Bayreuth) for the water uptake measurements as well as Lena Geiling (Electrochemical Process Engineering – University of Bayreuth) for the

help with the TGA measurements. We would like to thank Dr.-Ing. Daniel Leykam (Electrochemical Process Engineering – University of Bayreuth) for his help in preparing the graphical abstract. In addition, the help of the workshops at the University of Bayreuth is gratefully acknowledged.

## References

[1] A. Kusoglu, A.Z. Weber, Chem. Rev. 117 (2017) 987–1104.
[2] R. Stropnik, A. Lotrič, A. Bernad Montenegro, M. Sekavčnik, M. Mori, Energy Sci. Eng. 7 (2019) 2519–2539.
[3] M. Feng, R. Qu, Z. Wei, L. Wang, P. Sun, Z. Wang, Sci. Rep. 5 (2015) 1–8.
[4] P. Sreeraj, R. Vedarajan, N. Rajalakshmi, V. Ramadesigan, Int. J. Hydrogen Energy 46 (2021) 13020–13028.
[5] T. Stahl, D. Mattern, H. Brunn, Environ. Sci. Eur. 23 (2011) 1–52.
[6] T. Oki, T. Katsumata, K. Hashimoto, M. Kobayashi, Mater. Trans. 50 (2009) 1864–1870.
[7] N. Hoshi, M. Ikeda, Method for Recovering and Reusing Material for Solid High Polymer Fuel Cell, 1998, JPH11288732A.
[8] L. Shore, Process for Recycling Components of a PEM Fuel Cell Membrane Electrode Assembly, 2012. US 8124261 B2.
[9] M. Carmo, G.P. Keeley, D. Holtz, T. Grube, M. Robinius, M. Müller, D. Stolten, Int. J. Hydrogen Energy 44 (2019) 3450–3455.
[10] S. Grot, W. Grot, Recycling of Used Perfluorosulfonic Acid Membranes, 2007. US 7255798 B2.
[11] H.F. Xu, X. Wang, Z.G. Shao, I.M. Hsing, J. Appl. Electrochem. 32 (2002) 1337–1340.
[12] Q. Xu, X. Chen, S. Wang, C. Guo, Y. Niu, R. Zuo, Z. Yang, Y. Zhou, C. Xu, Energies 15 (2022) 8717.
[13] F. Xu, S. Mu, M. Pan, Int. J. Hydrogen Energy 35 (2010) 2976–2979.
[14] J. Koehler, R. Zuber, M. Binder, V. Baenisch, M. Lopez, Process for Recycling Fuel Cell Components Containing Precious Metals, 2010. US 7713502 B2.
[15] M. Laporta, M. Pegoraro, L. Zanderighi, Macromol. Mater. Eng. 282 (2000) 22–29.
[16] M.W. Muggli, G.D. Dahlke, D. Duchesne, T. Gerdes, P. Heimerdinger, K. Hintzer, S. Huber, M. Kutter, A. Rosin, C. Roth, A. Schmidt-Rodenkirchen, T.W. Schoettle, A. Thaler, F. Zentis, Process for Recycling a Solid Article Including a Fluorinated Polymer, 2023. WO 2023/111750 A1.
[17] G. Villalba, M. Segarra, A.I. Fernández, J.M. Chimenos, F. Espiell, Resour. Conserv. Recycl. 37 (2002) 39–53.
[18] M. Maier, D. Abbas, M. Komma, M.S. Mu'min, S. Thiele, T. Böhm, J. Membr. Sci. 669 (2023), 121244.
[19] Z. Peng, P. Huguet, S. Deabate, A. Morin, A.K. Sutor, J. Raman Spectrosc. 44 (2013) 321–328.
[20] P. Heimerdinger, A. Rosin, M.A. Danzer, T. Gerdes, Membranes 9 (2019) 62.
[21] G. Tsotridis, A. Pilenga, G. De Marco, T. Malkow, EU Harmonised Test Protocols for PEMFC-MEA Testing in Single Cell Configuration for Automotive Applications, 2015.
[22] G.A. Giffin, G.M. Haugen, S.J. Hamrock, V. Di Noto, J. Am. Chem. Soc. 135 (2013) 822–834.
[23] S. Mu, C. Xu, Q. Yuan, Y. Gao, F. Xu, P. Zhao, J. Appl. Polym. Sci. 129 (2013) 1586–1592.
[24] S.R. Samms, S. Wasmus, R.F. Savinell, J. Electrochem. Soc. 143 (1996) 1498.
[25] V. Di Noto, M. Piga, E. Negro, G.A. Giffin, S. Polizzi, T.A. Zawodzinski, RSC Adv. 3 (2013) 18960–18969.
[26] X. Luo, G. Lau, M. Tesfaye, C.R. Arthurs, I. Cordova, C. Wang, M. Yandrasits, A. Kusoglu, J. Electrochem. Soc. 168 (2021), 104517.
[27] Y. Li, R. Jiang, C. Gittleman, J. Power Sources 478 (2020), 228734.
[28] V.O. Kollath, Y. Liang, F.D. Mayer, X. Ma, C. Korzeniewski, K. Karan, J. Phys. Chem. C 122 (2018) 9578–9585.
[29] M. Danilczuk, L. Lin, S. Schlick, S.J. Hamrock, M.S. Schaberg, J. Power Sources 196 (2011) 8216–8224.
[30] R. Buzzoni, S. Bordiga, G. Ricchiardi, G. Spoto, A. Zecchina, J. Phys. Chem. 99 (1995) 11937–11951.
[31] A. Gruger, A. Régis, T. Schmatko, P. Colomban, Vib. Spectrosc. 26 (2001) 215–225.
[32] L. Ghassemzadeh, K.D. Kreuer, J. Maier, K. Müller, J. Power Sources 196 (2011) 2490–2497.
[33] L. Ghassemzadeh, M. Marrony, R. Barrera, K.D. Kreuer, J. Maier, K. Müller, J. Power Sources 186 (2009) 334–338.
[34] Q. Chen, K. Schmidt-Rohr, Macromolecules 37 (2004) 5995–6003.
[35] M. Robert, A. El Kaddouri, J.-C. Perrin, S. Leclerc, O. Lottin, J. Electrochem. Soc. 165 (2018) F3209–F3216.
[36] A. Kusoglu, T.J. Dursch, A.Z. Weber, Adv. Funct. Mater. 26 (2016) 4961–4975.
[37] Y. Tang, A.M. Karlsson, M.H. Santare, M. Gilbert, S. Cleghorn, W.B. Johnson, Mater. Sci. Eng., A 425 (2006) 297–304.
[38] L.M. Onishi, J.M. Prausnitz, J. Newman, J. Phys. Chem. B 111 (2007) 10166–10173.
[39] A. Kusoglu, S. Savagatrup, K.T. Clark, A.Z. Weber, Macromolecules 45 (2012) 7467–7476.
[40] J.T. Hinatsu, M. Mizuhata, H. Takenaka, J. Electrochem. Soc. 141 (1994) 1493–1498.
[41] G. Alberti, R. Narducci, M. Sganappa, J. Power Sources 178 (2008) 575–583.
[42] L. Maldonado, J.C. Perrin, J. Dillet, O. Lottin, J. Membr. Sci. 389 (2012) 43–56.
[43] Y. Liu, J.L. Horan, G.J. Schlichting, B.R. Caire, M.W. Liberatore, S.J. Hamrock, G. M. Haugen, M.A. Yandrasits, S. Seifert, A.M. Herring, Macromolecules 45 (2012) 7495–7503.
[44] L. Rubatat, A.L. Rollet, G. Gebel, O. Diat, Macromolecules 35 (2002) 4050–4055.
[45] K. Schmidt-Rohr, Q. Chen, Nat. Mater. 7 (2008) 75–83.
[46] T.D. Gierke, G.E. Munn, F.C. Wilson, J. Polym. Sci. Polym. Phys. Ed 19 (1981) 1687–1704.
[47] O. Fernihough, M.S. Ismail, A. El-kharouf, Membranes 12 (2022) 430.
[48] A. Stassi, I. Gatto, E. Passalacqua, V. Antonucci, A.S. Arico, L. Merlo, C. Oldani, E. Pagano, J. Power Sources 196 (2011) 8925–8930.